



university of  
 groningen

faculty of science  
 and engineering

---

# Current Sharing and Average Voltage Regulation of DC Microgrids under Communication Delays

---

*Bachelor Integration Project  
 Industrial Engineering and Management*

*Author:*

Irene Lulofs  
 s3332217

*Supervisors:*

Prof.dr.ir. J.M.A. Scherpen,  
 Dr. S. Feng,  
 Dr. A.J. Bosch

*June 4, 2021*



### **Abstract**

This Bachelor Integration Project introduces communication delays within a distributed control scheme for DC microgrids. The distributed control scheme without communication delays is designed to achieve two control objectives: current sharing and average voltage regulation. A distributed control system depends on exchanging measurements of connected local controllers via a communication network. By introducing communication delays that may occur in the communication between controllers, the performance of the controller is evaluated. Simulations with constant delays over one of the subjected parameters indicate that the system shows robustness against delays to some extent. However, when delays are simulated over both parameters, the system is robust only to small delays and thus needs further improvement to validate stability and reliability under the influence of communication delays.

# Contents

<b>List of Figures</b>	<b>iv</b>
<b>List of Tables</b>	<b>v</b>
<b>1 Introduction</b>	<b>1</b>
1.1 Introduction to microgrids . . . . .	1
1.2 Thesis Outline . . . . .	2
<b>2 Problem Analysis</b>	<b>3</b>
2.1 Problem context . . . . .	3
2.2 System description . . . . .	3
2.3 Stakeholder analysis . . . . .	3
2.4 Problem statement . . . . .	3
<b>3 Research Focus</b>	<b>4</b>
3.1 Research Goal . . . . .	4
3.2 Research Questions . . . . .	4
3.3 Research Strategy . . . . .	4
<b>4 Validation</b>	<b>5</b>
<b>5 Theoretical Framework</b>	<b>6</b>
5.1 Model description . . . . .	6
5.2 Mathematical model . . . . .	7
5.3 Control objectives . . . . .	8
5.4 Control scheme . . . . .	8
5.5 Used parameters . . . . .	9
5.5.1 Modeling . . . . .	9
<b>6 Communication Network and its Delays</b>	<b>10</b>
6.1 Communication network principle . . . . .	10
6.2 Communication delays . . . . .	11
<b>7 Communication Delay Implementation</b>	<b>12</b>
7.1 Constant communication delays over $I_t$ measurements . . . . .	12
7.1.1 Simulation results . . . . .	12
7.2 Constant communication delays over $\theta$ measurements . . . . .	15
7.2.1 Simulation results . . . . .	15
7.3 Constant communication delays over $I_t$ and $\theta$ measurements . . . . .	18
7.3.1 Simulation results . . . . .	18
<b>8 Results</b>	<b>21</b>
8.1 Constant communication delays in $I_t$ measurements . . . . .	21

8.1.1	Scenario 1 . . . . .	21
8.1.2	Scenario 2 . . . . .	21
8.2	Constant communication delays in $\theta$ measurements . . . . .	21
8.2.1	Scenario 1 . . . . .	21
8.2.2	Scenario 2 . . . . .	21
8.3	Constant communication delays in $I_t$ and $\theta$ measurements . . . . .	22
8.3.1	Scenario 1 and Scenario 2 . . . . .	22
8.3.2	Scenario 3 . . . . .	22
<b>9</b>	<b>Discussion</b>	<b>23</b>
<b>10</b>	<b>Conclusion</b>	<b>24</b>
	<b>Bibliography</b>	<b>25</b>
<b>A</b>	<b>Modeling without delays</b>	<b>27</b>
A.1	Simulink model . . . . .	27
A.2	Plots of generated currents, voltages, and line currents . . . . .	28
<b>B</b>	<b>Modeling with delays</b>	<b>29</b>
B.1	Simulink model with delays . . . . .	29

## List of Figures

5.1	Electrical scheme of DGU $i$ and line $k$ (Trip et al., 2018) . . . . .	6
5.2	Scheme of considered microgrid with communication network (Trip et al., 2018)	6
6.1	Communication between two nodes . . . . .	10
6.2	Communication lines between the different nodes . . . . .	10
7.1	Simulation results $I_t$ , $\tau = 20ms$ . . . . .	13
7.2	Simulation results $I_t$ , $\tau = 200ms$ . . . . .	14
7.3	Simulation results $\theta$ , $\tau = 20ms$ . . . . .	16
7.4	Simulation results $\theta$ , $\tau = 200ms$ . . . . .	17
7.5	Simulation results, $\tau = 20ms$ and $\tau = 200ms$ . . . . .	19
7.6	Simulation results, $\tau = 2ms$ . . . . .	20
A.1	Overview of the used Simulink model (based on the article by Trip et al. (2018))	27
A.2	Simulation results (based on the article by Trip et al. (2018)) . . . . .	28
B.1	Overview of the used Simulink model with delays . . . . .	29
B.2	Detailed overview of modeled delay over $I_t$ . . . . .	30
B.3	Detailed overview of modeled delay over $\theta$ . . . . .	30

## List of Tables

5.1	Description of the used symbols . . . . .	7
5.2	Microgrid parameters . . . . .	9

# Chapter 1: Introduction

## 1.1 Introduction to microgrids

The electric power system is the most complex managed power system. As demand increases per year and the conventional energy sources gradually exhaust, an alternative energy source to sustain the growth of power generation in the future is required (Kaur et al., 2016).

Solutions entail implementing a cluster of loads and micro sources operating as a single local controllable system (Delfino et al., 2018). In general, such a cluster is defined as a microgrid and is a low voltage electrical distribution network, composed of Distributed Generation Units (DGUs), loads, and storage systems interconnected through power lines (Cucuzzella et al., 2018). Renewable energy sources (RESs) are implied mostly as small scale DGUs in microgrids (Kotpalliwar et al., 2015). The microgrid can either be connected to the main power grid, or operate in isolated mode reliant on its own generation capacity (Saleh et al., 2018).

Most microgrids have been implemented as Alternate Current (AC) microgrids as they match the characteristics of the conventional AC grid. AC microgrids are a logical consequence of the extensive experience with large AC grids, the wide availability of AC loads, and the maturity of the inverter industry in converting Direct Current (DC) power into AC power (Zubieta, 2016).

However, many sources and loads (e.g. photovoltaic panels, batteries, and electronic appliances) can be directly connected to DC microgrids by using DC-DC converters, making DC microgrids in some situations more efficient than AC microgrids (Trip et al., 2018). Because of their reduced complexity, DC microgrids are often deployed where reliability is essential (Zubieta, 2016).

In literature, two control problems of DC microgrids have been addressed and are respectively (1) current sharing, and (2) average voltage regulation. Current sharing within the microgrid prevents the overstressing of any source. It is desired that the total demand of the network is shared among all the various DGUs proportionally to the generation capacity of their corresponding energy sources (Trip et al., 2018). Moreover, regulating the voltages is required to ensure the proper functioning of connected loads (Cucuzzella et al., 2018). In particular, achieving both objectives simultaneously has proven to be a challenge. However, in Trip et al. (2018) a distributed control scheme is proposed which achieves *both* current sharing and average voltage regulation. These objectives are achieved independently of the initial condition of the controlled microgrid, require only measurements of the generated currents (no voltage measurements are needed), are independent of the microgrid parameters, and the topology of the used communication network.

Communication networks are implemented in distributed controllers to exchange local measurements between neighboring nodes to control the system more locally than centrally. This network consists of multiple communication lines between the connected nodes (Trip et al., 2018). That said, when data is exchanged via a communication network, the system is inevitably exposed to potential time delays as it always suffers from communication limitations (Ding et al., 2018). Therefore, it is important to include these delays at the design stage of the controller to ensure reliable and stable performance.

## 1.2 Thesis Outline

The structure of this thesis is as follows: in chapter 2, the problem context, the system description, stakeholders in the research and the problem statement are covered. Subsequently, the research goal and questions are discussed in chapter 3, as well as the strategy of this research. The validation of the research is addressed in chapter 4.

Chapter 5 introduces the mathematical model considered in this research and includes the control objectives which will evaluate whether the system under communication delays, introduced in 6 and simulated in chapter 7, is operating within expectations. In chapter 8 and 9, the performance of the controller is evaluated and afterwards discussed. Chapter 10 concludes the outcome of this thesis.

## Chapter 2: Problem Analysis

### 2.1 Problem context

As stated in chapter 1, distributed controllers of DC microgrids face two control problems. Trip et al. (2018) has proposed a control scheme for DC microgrids which achieves both problems simultaneously, meaning that the controller is able to achieve current sharing and average voltage regulation.

All connected DGUs have to be properly controlled to manage the bidirectional power exchange to accommodate the excessive DC demands with minimal power disruptions or load shedding (Radwan and Mohamed, 2014). As this coordination is dependent on communication across the resources, potential influences on communication must be considered. One of the main influences of such a communication network is possible delays that may occur in a communication line, resulting in a delay in the exchange of measurements to and from different DGUs. The proposed controller, however, does not include the influence of communication delays.

### 2.2 System description

This research is build upon the proposed distributed control scheme of a DC microgrid in Trip et al. (2018). The mathematical models and parameters of the article are elaborated on in chapter 5. Under the influence of delays in the communication network, this project will first modify the proposed control scheme to include these delays. Afterwards, it will be purely investigated if the controller is able to distribute the power to satisfy the demand by means of the control objectives mentioned in chapter 1.1.

### 2.3 Stakeholder analysis

The first stakeholder of this Bachelor Integration Project is prof.dr.ir. J.M.A. Scherpen. The research conducted in this project lies within the focus of the Discrete Technology Production Automation (DTPA) research group, of which she is chair. Besides, the control scheme on which this project is based was co-authored by her, making her a primary stakeholder.

The second stakeholder is dr. S. Feng. He is a post-doctoral researcher of the DTPA research group and is the daily supervisor of this integration project. As daily supervisor, he has a significant level of influence on the direction of the project and is thus considered an important stakeholder.

### 2.4 Problem statement

The following problem statement is derived:

*As a microgrid can include DGUs with different generation capacity, proper coordination among the DGUs is required. Exchanging measurements of these connected DGUs requires a communication network within the microgrid. The proposed DC microgrid control scheme by Trip et al. (2018) includes the communication network, however, does not include the possibility of delays occurring in the communication lines. In order to operate as reliable as possible in terms of current sharing and average voltage control throughout the grid, these influences should be included in the control scheme.*

## Chapter 3: Research Focus

### 3.1 Research Goal

The goal of this research is to include communication delays in the distributed control scheme developed in Trip et al. (2018). The modified control scheme should still achieve its control objectives of current sharing and average voltage control under these delays. Performance of the modified control scheme will be validated by means of simulations. The research should be realised within a period of 2 months.

### 3.2 Research Questions

Based on the problem analysis performed in chapter 2 and the research goal stated in chapter 3.1, the main research question is constructed as follows:

1. **”Does the proposed controller developed in Trip et al. (2018) still achieve its control objectives when adjusted in its design in order to include communication delays?”**
  - (a) To what extent influence communication delays the controller’s performance?
  - (b) In what way can the influences of communication delays be implemented in the proposed controller?
  - (c) Does the controller, which includes the communication delays, still achieve its control objectives?

### 3.3 Research Strategy

Three key decisions are taken in order to make a solid choice for a research strategy (Verschuren et al., 2010):

1. Breadth vs. depth: This research is associated as a depth research. The research is aimed to modify a control scheme for a DC microgrid. This could be considered a small-scale approach.
2. Qualitative vs. quantitative research: This research will include a qualitative research as the implementation of communication delays is included in one specific distributed control scheme.
3. Empirical vs. desk research: The testing of a controller requires values for its parameters, however, this data will not be collected in reality but is related to it and mentioned in the considered article by Trip et al. (2018). Besides, desk research is conducted to fully grasp all aspects when modifying a controller.

Based on these three decisions, it is concluded that a case study is performed. The comparative case study is considered, as the research will both focus on analysing the microgrid control scheme when including time delays in the communication network, as well as an ideal controller to compare performance of the controller. The research will include mathematical modeling and data analysis with the tools Matlab and Simulink.

## Chapter 4: Validation

The final deliverable of this research, i.e. the artifact, is a validation whether the proposed control scheme of a DC microgrid in Trip et al. (2018) still reaches its control objectives under the influence of communication delays.

The validity of this study can be ensured by initially replicating the control scheme of Trip et al. (2018) and testing the robustness of the model through simulations. Moreover, the modified control scheme is also evaluated in this research. This is carried out by first simulating the behaviour of the control scheme when delays are introduced. Analysis of the simulations afterwards will justify whether, with the modifications made to the controller proposed in Trip et al. (2018), the system still meets the objectives of current sharing and average voltage regulation.

## Chapter 5: Theoretical Framework

### 5.1 Model description

The microgrid model that is considered in this project is defined and formulated by Trip et al. (2018). The model describes a typical DC microgrid composed of  $n$  DGUs connected to each other through  $m$  resistive-inductive (RL) power lines.

The energy source of each DGU is represented by a DC voltage source that supplies a local load through a DC-DC buck converter. The local DC load is connected to the so-called Point of Common Coupling (PCC) (Trip et al., 2018). Besides, a current sensor, inductor, resistor, capacitor, load resistor and a voltage sensor are included in the model. The power transmission line consists of an inductor and resistor. The described set-up of a DGU can be found in Figure 5.1.

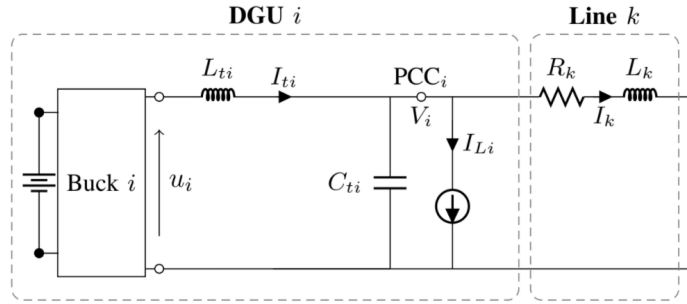


Figure 5.1: Electrical scheme of DGU  $i$  and line  $k$  (Trip et al., 2018)

The complete scheme of the microgrid considered in this research consists of 4 interconnected DGUs and 4 resistive-inductive power lines, which is shown in Figure 5.2. Moreover, the blue dashed lines represent the communication lines between nodes of the microgrid. Further elaboration on the communication network is provided in chapter 6.1.

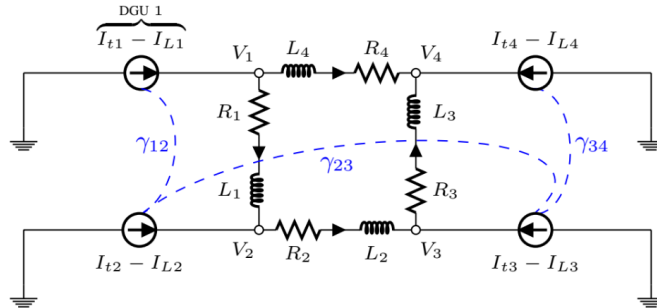


Figure 5.2: Scheme of considered microgrid with communication network (Trip et al., 2018)

## 5.2 Mathematical model

The model as described above is mathematically justified by Trip et al. (2018). For DGU  $i$ , the following equations characterize its dynamic behaviour:

$$L_{ti}\dot{I}_{ti} = -V_i + u_i \quad (5.1)$$

$$C_{ti}\dot{V}_i = I_{ti} - I_{Li} - \sum_{k \in \varepsilon_i} I_k, \quad (5.2)$$

where  $\varepsilon_i$  is the set of power lines incident to the DGU  $i$ . The control input  $u_i$  represents the buck converter output voltage. Moreover, the current from DGU  $i$  to DGU  $j$  is denoted by  $I_k$ , and its dynamic equation is given by

$$L_k\dot{I}_k = (V_i - V_j) - R_k I_k \quad (5.3)$$

The symbols used in (5.1), (5.2), and (5.3) are displayed in table 5.1.

State variables	
$I_{ti}$	Generated current
$V_i$	Load voltage
$I_k$	Line current
Parameters	
$L_{ti}$	Filter inductance
$C_{ti}$	Shunt capacitor
$R_k$	Line resistance
$L_k$	Line inductance
Inputs	
$u_i$	Control input
$I_{Li}$	Unknown current demand

Table 5.1: Description of the used symbols

The overall network of DGUs and power lines is represented by a connected and undirected graph  $\mathcal{G} = (\mathcal{V}, \mathcal{E})$ , where the nodes,  $\mathcal{V} = \{1, \dots, n\}$ , represent the DGUs and the edges,  $\mathcal{E} = \{1, \dots, m\}$ , represent the power lines interconnecting the DGUs. The network topology is represented by its corresponding incidence matrix  $\mathcal{B} \in \mathbb{R}^{n \times m}$ . The ends of edge  $k$  are arbitrarily labeled with a + and a -, and the entries of  $\mathcal{B}$  are given by

$$\mathcal{B}_{ik} = \begin{cases} +1 & \text{if } i \text{ is the positive end of } k \\ 1 & \text{if } i \text{ is the negative end of } k \\ 0 & \text{otherwise.} \end{cases}$$

### 5.3 Control objectives

The two control objectives to be achieved by the proposed control scheme are current sharing and average voltage regulation. These two objectives are mathematically expressed in the following equations:

$$\lim_{t \rightarrow \infty} I_t(t) = \bar{I}_t = W^{-1} \mathbb{1} i_t^* \quad (5.4)$$

$$\lim_{t \rightarrow \infty} \mathbb{1}^T W^{-1} V(t) = \mathbb{1}^T W^{-1} \bar{V} = \mathbb{1}^T W^{-1} V^* \quad (5.5)$$

Current sharing is formulated in (5.4) where  $W = \text{diag}(w_1, \dots, w_n)$ ,  $w_i > 0$  and  $i_t^* = \frac{\mu^T I_L}{\mu^T W^{-1} \mu}$ . (Proportional) current sharing is achieved when  $w_i I_{ti} = w_j I_{tj}$  for all  $i, j \in \mathcal{V}$ , where a relatively large value of  $w_i$  corresponds to a relatively small generation capacity of DGU  $i$ .

Average voltage control is formulated in (5.5) where the weighted average value of the steady state voltage ( $\bar{V}$ ) of all DGUs is identical to the weighted average value of the desired voltage ( $V^*$ ).

### 5.4 Control scheme

Trip et al. (2018) considers a distributed controller at node  $i \in \mathcal{V}$  of the form:

$$T_{\theta i} \dot{\theta}_i = - \sum_{j \in \mathcal{N}_i^{\text{com}}} \gamma_{ij} (w_i I_{ti} - w_j I_{tj}) \quad (5.6)$$

$$T_{\phi i} \dot{\phi}_i = -\phi_i + I_{ti} \quad (5.7)$$

$$u_i = -K_i (I_{ti} - \phi_i) + w_i \sum_{j \in \mathcal{N}_i^{\text{com}}} \gamma_{ij} (\theta_i - \theta_j) + V_i^* \quad (5.8)$$

The parameters  $T_{\theta i}, T_{\phi i}, K_i \in \mathbb{R}_{>0}$  permit appropriate tuning of the transient response. The set  $\mathcal{N}_i^{\text{com}}$  is the set of nodes connected to node  $i$  via a communication network, with edge weights  $\gamma_{ij} = \gamma_{ji} \in \mathbb{R}_{>0}$ . The overall communication network is, similar to the topology of the microgrid, represented by a connected and undirected graph  $\mathcal{G}^{\text{com}} = (\mathcal{V}^{\text{com}}, \mathcal{E}^{\text{com}})$ , where  $\mathcal{V}^{\text{com}} = \mathcal{V}$  and the edges,  $\mathcal{E}^{\text{com}} = \{1, \dots, m\}$ , represent the communication links between the DGUs. The communication network topology is described by its corresponding incidence matrix  $\mathcal{B}^{\text{com}} \in \mathbb{R}^{n \times m_c}$ , which is defined similarly as  $\mathcal{B}$ .

Resulting from equations (5.6)-(5.8), the overall control scheme can be written for all  $i \in \mathcal{V}$ :

$$T_{\theta} \dot{\theta} = -\mathcal{L}^{\text{com}} * W * I_t \quad (5.9)$$

$$T_{\phi} \dot{\phi} = -\phi + I_t \quad (5.10)$$

$$u = -K(I_t - \phi) + W * \mathcal{L}^{\text{com}} * \theta + V_i^*, \quad (5.11)$$

where  $T_{\theta}, T_{\phi}, K \in \mathbb{R}^{n \times n}$  are positive definite diagonal matrices. Furthermore,  $\mathcal{L}^{\text{com}}$  is the (weighted) Laplacian matrix associated to the communication network.

## 5.5 Used parameters

Table 5.2 shows the used parameters in modeling the controller, stated in Cucuzzella et al. (2018).

DGU		1	2	3	4
$L_{ti}$	(mH)	1.8	2.0	3.0	2.2
$C_{ti}$	(mF)	2.2	1.9	2.5	1.7
$w_i$	(-)	$0.4^{-1}$	$0.2^{-1}$	$0.15^{-1}$	$0.25^{-1}$
Lines		{1,2}	{2,3}	{3,4}	{1,4}
$R_k$	(m $\Omega$ )	70	50	80	60
$L_k$	( $\mu H$ )	2.1	2.3	2.0	1.8

Table 5.2: Microgrid parameters

### 5.5.1 Modeling

Based on the mathematical model (chapter 5.2) and the proposed control scheme (chapter 5.4), the general Simulink model of the system is depicted in Figure A.1. For simulation analysis and comparison, the generated currents and voltages of the DGUs are depicted in Figure A.2a and A.2b. The currents in the lines in between the DGUs can be viewed in Figure A.2c.

## Chapter 6: Communication Network and its Delays

### 6.1 Communication network principle

As stated in chapter 5, the communication network within the microgrid consists of several communication lines between the interconnected DGUs. The communication lines ensure that local measurements are exchanged through the microgrid.

The distributed control scheme of a DGU, stated in equations (5.6) - (5.8), does not require any voltage measurements from the connected nodes. However, as can be specifically seen in equation (5.6), DGU  $i$  does require  $I_t$  measurements of DGU  $j$  in order to calculate its  $\theta_i$  value. In addition, equation (5.8) shows that DGU  $i$  needs DGU  $j$  its  $\theta$  measurements in order to compute  $u_i$ . Concluding, the distributed controllers prescribe a communication network to exchange information on the generated current ( $I_t$ ) and the value of  $\theta$  among neighboring nodes. The principle of communication between two nodes is depicted in Figure 6.1.

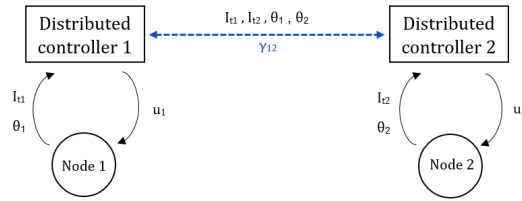


Figure 6.1: Communication between two nodes

Each distributed controller receives measurements ( $I_t$  and  $\theta$ ) of the node and transmits the controller output ( $u$ ) back to the system. The dashed line in Figure 6.1 depicts the communication line through which information is exchanged between the two nodes. This communication is key to achieve the control objectives current sharing (5.4) and average voltage regulation (5.5). In Figure 6.2 the communication lines in the considered microgrid are depicted with the blue dashed lines (simplified version of Figure 5.2),  $k_{ij}$  represent the power lines.

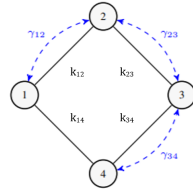


Figure 6.2: Communication lines between the different nodes

Following from this figure, the incidence matrix ( $\mathcal{B}^{com}$ ) of the communication network can be obtained:

$$\mathcal{B}^{com} = \begin{pmatrix} -1 & 0 & 0 \\ 1 & -1 & 0 \\ 0 & 0 & 1 \end{pmatrix}$$

## 6.2 Communication delays

As previously mentioned, the main dependency of a distributed control system is that it needs support from a communication network to exchange local measurements between DGUs.

The main problem, however, is that time delays are typically present in systems that must communicate over a network. This is mainly because delays in communication lines impede the transmission of information and will affect the performance of all connected nodes (Allen-Prince et al., 2017). In addition, the distributed control scheme of this project requires bidirectional interactions which adds to the complexity of the time delay (Dong et al., 2017).

Delays in the network can lead to unpredictable behavior of the microgrid system and are impossible to ignore (Allen-Prince et al., 2017). If not dealt with in the design phase, time delays can lead to instability of the microgrid (Khalil et al., 2016).

Time delays in microgrid systems have been investigated in many articles. Several methods have been proposed to incorporate these delays into control systems. However, the literature has mainly focused on communication delays between different control layers: (Baros et al., 2020), (Han et al., 2017), (Dong et al., 2017), and (Khalil et al., 2016). Delays between local controllers and the microgrid central controller have also been mentioned in several articles: (Saleh et al., 2018), (Ustun et al., 2012), and (Macana et al., 2013).

In order to include communication delays in the specific distributed control scheme by Trip et al. (2018), the methodologies of all the articles mentioned are observed. Chapter 7 explains the strategy used in this project. For analysis purposes, communication delays between neighboring nodes are assumed to have the same, constant delay.

The values of the delays in this project are based on various statements in articles. Normally, as stated by Ustun et al. (2012), the communication delays occurring in microgrids are of milliseconds range. In Du et al. (2018), expected ranges of time delays are summarized based on real-time network traffic data. Cited articles in this chapter mainly apply delays in the range of 1 – 300ms and thus will be set as limits of the delays described in chapter 7.

## Chapter 7: Communication Delay Implementation

### 7.1 Constant communication delays over $I_t$ measurements

In this section, constant time delays will be modeled over  $I_t$  measurements to analyze the system's stability.

When considering DGU  $i$ , one can observe in equation (5.6) that measurements of  $I_{tj}$  (its neighboring node) are required and will thus be exchanged via the communication network. Delays only occur over transmitted measurements from other nodes and not from the specific node itself. As can be seen in Figure 6.2, several DGUs will exchange data with multiple DGUs.

To demonstrate how the communication delays will be simulated in the model, a mathematical modification to equation (5.11) is given in (7.1) specifically for DGU 1. The same general concept will be applied to all DGUs.

$$T_{\theta_1} \dot{\theta}_1 = -\mathcal{L}_{com} * W * \begin{bmatrix} I_{t1}(t) \\ I_{t2}(t - \tau) \\ I_{t3}(t - \tau) \\ I_{t4}(t - \tau) \end{bmatrix} \quad (7.1)$$

The following time delays ( $\tau$ ) occurring in the communication lines are simulated:

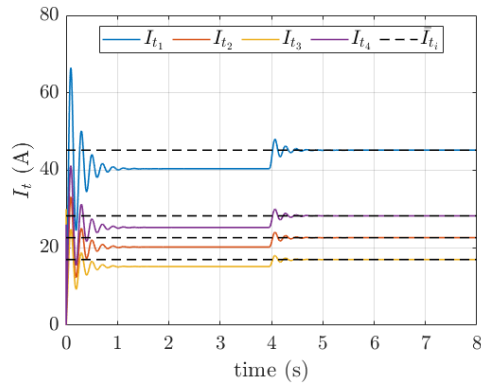
- Scenario 1:  $20ms$
- Scenario 2:  $200ms$

#### 7.1.1 Simulation results

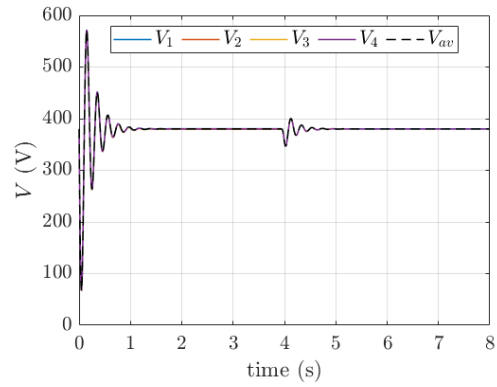
In Figure 7.1, the simulation results of scenario 1 are shown. Figure 7.2 shows the results of the second scenario. Figures 7.1a and 7.2a show the generated currents in the DGUs. Figure 7.1b and 7.2b represent the voltages in the DGUs. Lastly, the current in the lines between the DGUs are depicted in Figure 7.1c and 7.2c. Figure B.2 shows the detailed overview of the Simulink model with delays over  $I_t$  measurements.

The interpretation of results will be elaborated on in chapter 8.

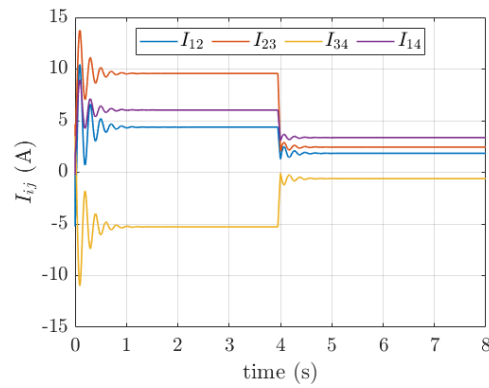
## Scenario 1



(a) Plot of the generated currents in the DGUs



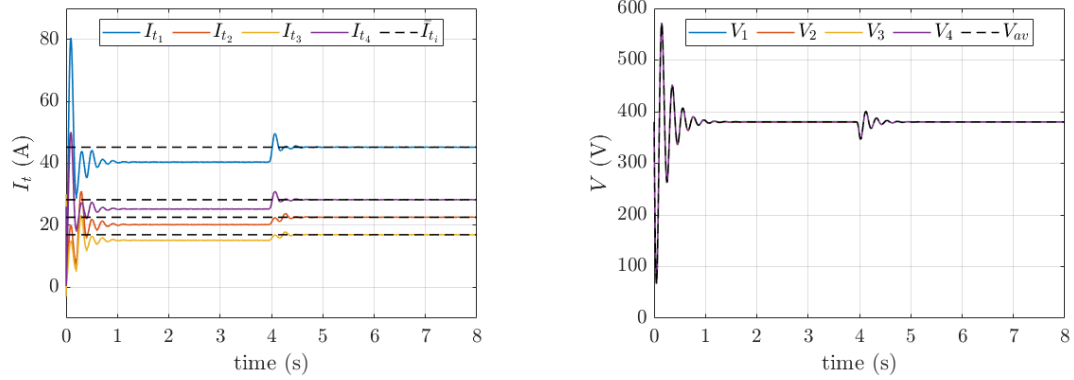
(b) Plot of the voltages in the DGUs



(c) Plot of the current in the line between the DGUs

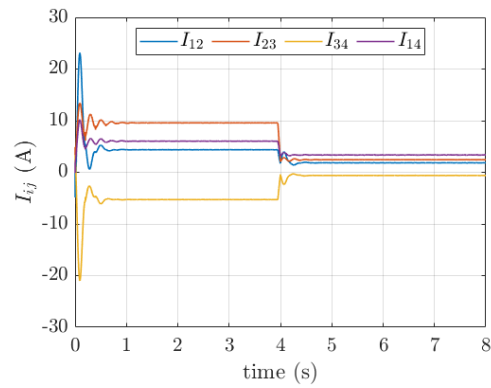
Figure 7.1: Simulation results  $I_t$ ,  $\tau = 20ms$

## Scenario 2



(a) Plot of the generated currents in the DGUs

(b) Plot of the voltages in the DGUs



(c) Plot of the current in the line between the DGUs

Figure 7.2: Simulation results  $I_t$ ,  $\tau = 200ms$

## 7.2 Constant communication delays over $\theta$ measurements

In this section, constant time delays will be modeled over  $\theta$  measurements to analyze the system's stability. The  $I_t$  measurements are considered ideal: no delays are modeled over these measurements.

When considering DGU  $i$ , one can observe in equation (5.8) that measurements of  $\theta_j$  (its neighboring node) are required and will thus be exchanged via the communication network. A similar mathematical formulation as in chapter 7.1 is provided to simulate the delays. For DGU 1, the following equation is considered:

$$u_1 = -K(I_t - \phi) + W * \mathcal{L}_{com} * \begin{bmatrix} \theta_1(t) \\ \theta_2(t - \tau) \\ \theta_3(t - \tau) \\ \theta_4(t - \tau) \end{bmatrix} + V^* \quad (7.2)$$

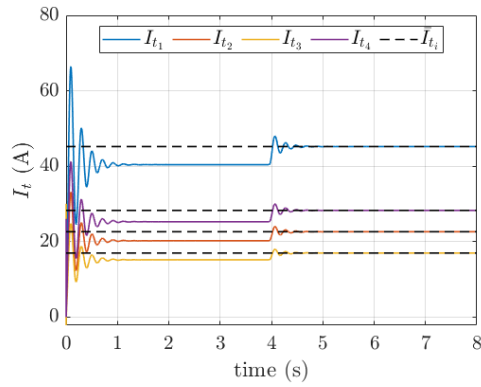
The following time delays ( $\tau$ ) occurring in the communication lines are simulated:

- Scenario 1:  $20ms$
- Scenario 2:  $200ms$

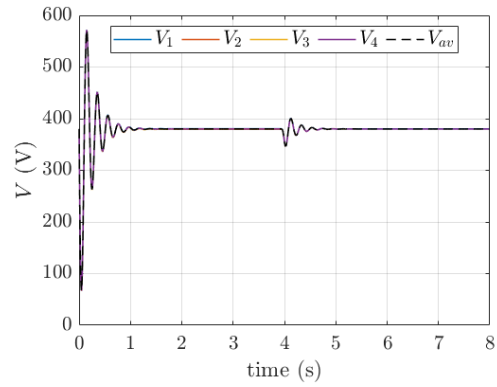
### 7.2.1 Simulation results

The results of the first scenario are depicted in 7.3, and of scenario 2 in 7.4. The generated currents can be view in 7.3a and 7.4a. Voltages in the DGUs are shown in 7.3b and 7.4b. Figure 7.3c and 7.4c plot the line currents between the DGUs. Figure B.3 shows the modified Simulink model in order to include the different delays over  $\theta$  measurements. Further interpretation of the results will be elaborated on in chapter 8.

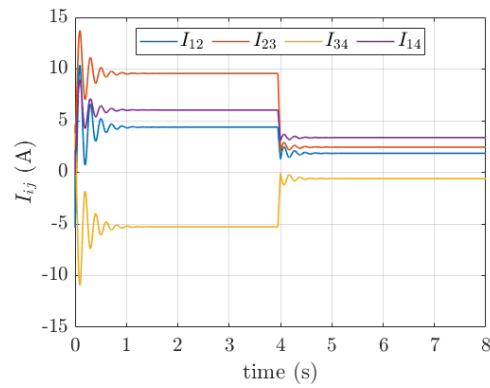
## Scenario 1



(a) Plot of the generated currents in the DGUs



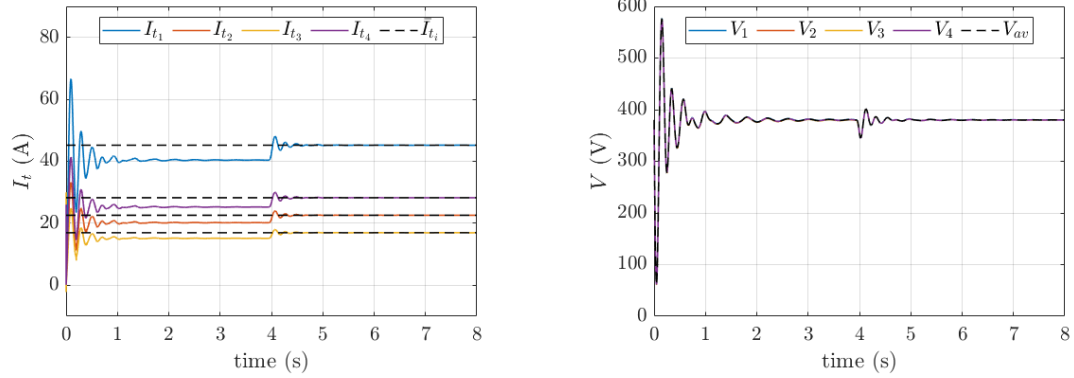
(b) Plot of the voltages in the DGUs



(c) Plot of the current in the line between the DGUs

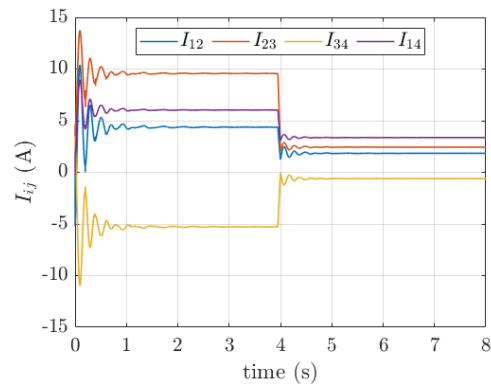
Figure 7.3: Simulation results  $\theta$ ,  $\tau = 20ms$

## Scenario 2



(a) Plot of the generated currents in the DGUs

(b) Plot of the voltages in the DGUs



(c) Plot of the current in the line between the DGUs

Figure 7.4: Simulation results  $\theta$ ,  $\tau = 200ms$

### 7.3 Constant communication delays over $I_t$ and $\theta$ measurements

In this section, both modeled delays of chapter 7.1 and 7.2 are combined in order to simulate a time delay throughout the whole model and observe the system's stability.

The following time delays ( $\tau$ ) of  $I_t$  and  $\tau$  are simulated:

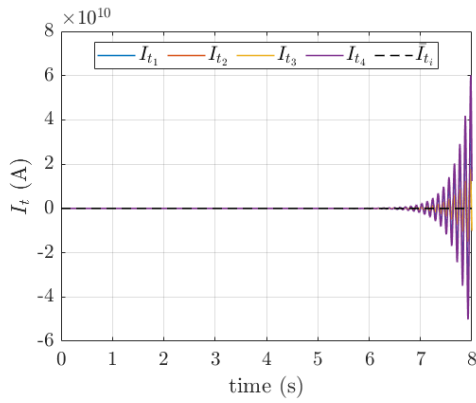
- Scenario 1:  $20ms$  per measurement
- Scenario 2:  $200ms$  per measurement
- Scenario 3:  $2ms$  per measurement

#### 7.3.1 Simulation results

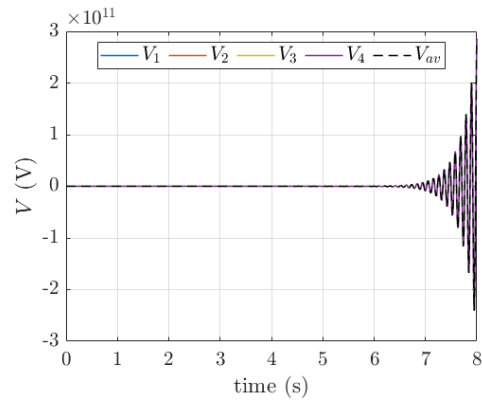
As scenario 1 and scenario 2 show similar exponential behavior, it is decided to include plots from one scenario instead of both.

Plots from scenario 1 and 2 can be observed in Figure 7.5, scenario 3 in Figure 7.6. Generated currents be found in Figure 7.5a and 7.6a, whereas the voltages in the DGUs are depicted in Figure 7.5b and 7.6b. The current in the lines between the DGUs are shown in Figure 7.5c and 7.6c. The overall Simulink model used to simulate these plots can be found in Figure B.1.

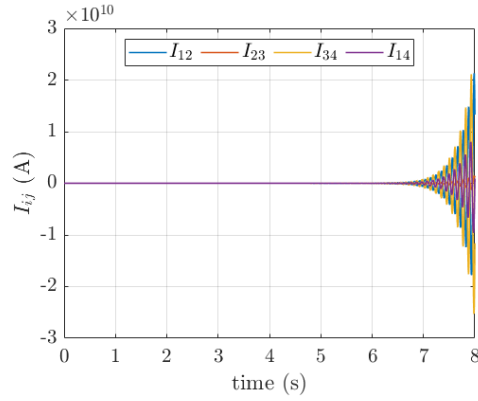
**Scenario 1 and Scenario 2**



(a) Plot of the generated currents in the DGUs



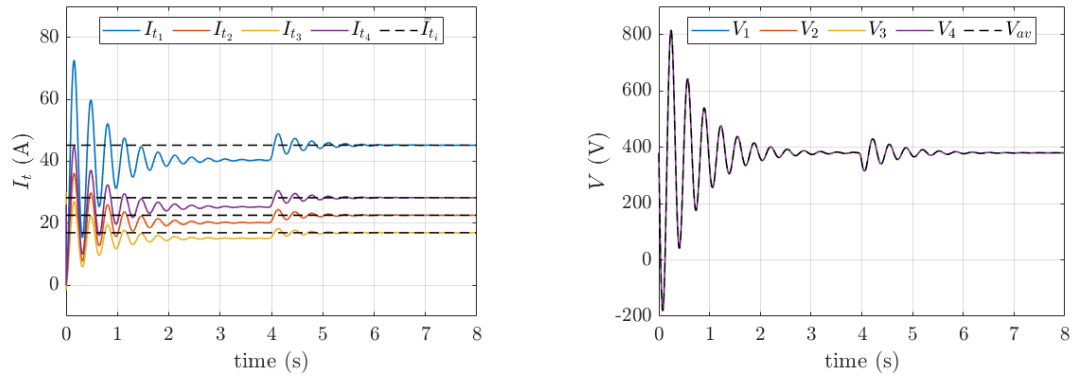
(b) Plot of the voltages in the DGUs



(c) Plot of the current in the line between the DGUs

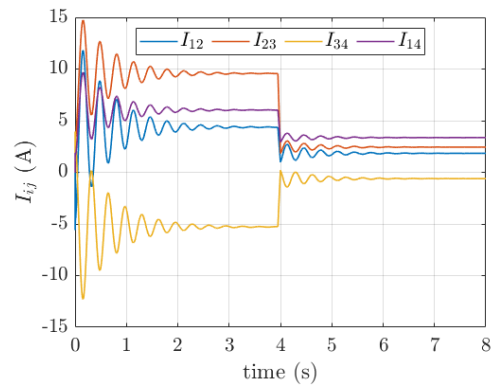
Figure 7.5: Simulation results,  $\tau = 20ms$  and  $\tau = 200ms$

## Scenario 3



(a) Plot of the generated currents in the DGUs

(b) Plot of the voltages in the DGUs



(c) Plot of the current in the line between the DGUs

Figure 7.6: Simulation results,  $\tau = 2ms$

## Chapter 8: Results

### 8.1 Constant communication delays in $I_t$ measurements

#### 8.1.1 Scenario 1

Figure 7.1a shows the generated currents of each DGU along with the corresponding values (dashed lines) corresponding to (proportional) current sharing for  $t > 1$ . Moreover, Figure 7.1c shows that current is flowing from one DGU to another. It can be observed that the current is balanced between the nodes and, according to equation (5.4), the objective of current sharing is achieved.

The steady state voltage is achieved after one second for both the initial start of the simulation and after the variation in  $I_L$  at  $t = 4$  as observed in Figure 7.1b. As the weighted average steady state voltage of the graph equals the reference voltage (380V), it is concluded that average voltage regulation is achieved according to equation (5.5). Moreover, it can be seen that when the generated currents increase, the voltage exhibits an opposite behavior.

#### 8.1.2 Scenario 2

The influence of  $\tau = 200ms$  compared to  $\tau = 20ms$  in scenario 1 can be observed in greater oscillations in the generated current plot (Figure 7.2a) and in the line current plot (Figure 7.2c). It can, however, be concluded that as current is shared between the DGUs, and the generated currents reach its (proportional) steady state value, the current sharing objective 5.4 is achieved.

The voltages in the DGUs (Figure 7.2b) show the same behavior as described in scenario 1 (8.1.1). It is concluded that average voltage sharing, stated in equation (5.5), is achieved.

### 8.2 Constant communication delays in $\theta$ measurements

#### 8.2.1 Scenario 1

The results of simulating  $\tau = 20ms$  over  $\theta$  measurements, equal the results of simulating  $\tau = 20ms$  over  $I_t$  measurements (8.1.1):

The currents generated in the DGUs are depicted in Figure 7.3a. Together with the line currents (Figure 7.3c), one can observe that current is shared between the nodes and that, according to equation (5.4), current sharing is achieved.

The steady state voltage is achieved after one second for both the initial start of the simulation and after a variation in  $I_L$  at  $t = 4$  as observed in Figure 7.3b. As the weighted average steady state voltage equals the  $V^*$  (380V), it is concluded that average voltage regulation is achieved according to equation (5.5).

#### 8.2.2 Scenario 2

The influence of  $\tau = 200ms$  compared to  $\tau = 20ms$  in scenario 1 is quite similar to scenario 1 (8.2.1). It can be observed that a greater delay in  $\theta$  measurements, does not influence the deviation in oscillations in the generated current plot (Figure 7.4a) and in the line current plot (Figure 7.4c). However, the system does take a slightly longer time to reach its steady state.

It can be concluded that, as current is shared between the DGUs and the generated currents reach its (proportional) steady state value, that the current sharing objective, equation 5.4, is achieved.

In addition, compared to the generated currents when applying the same delay over the  $I_t$  measurements (Figure 7.2a), it is concluded that a delay over  $I_t$  measurements has a greater impact on the generated currents in the DGUs compared to a delay over  $\theta$  measurements. This can be validated as  $I_t$  measurements are required in both equation (5.9) and (5.11), whereas  $\theta$  measurements are solely included in (5.11); limiting its influence on the overall system's performance to some extent.

The voltages in the DGUs (Figure 7.4b) show the same behavior as described in scenario 1 (8.2.1). It is therefore again concluded that average voltage sharing is achieved.

### 8.3 Constant communication delays in $I_t$ and $\theta$ measurements

#### 8.3.1 Scenario 1 and Scenario 2

As can be seen in Figure 7.5, the system its dynamics are exponentially increasing per time step when implementing  $\tau = 20ms$  and  $\tau = 200ms$ . Neither of the control objectives are achieved and it is apparent that with these delays, the distributed control system cannot achieve the optimal solution and is, in fact, unstable.

#### 8.3.2 Scenario 3

Figure 7.6 shows the results of the simulation when both measurements are subjected to  $\tau = 2ms$ . One can observe the generated current plot and the line current plot. The line current plot illustrates that current is flowing from one DGU to another. According to equation (5.4), it can be concluded that current sharing is achieved. Besides, delays over both measurements require a slightly longer time to reach the system's steady state. In addition, oscillations are increasing as well, which is unfavorable behavior in terms of reliability.

Moreover, Figure 7.6b shows the voltages in the DGUs. After approximately 3 seconds, average voltage control is achieved. At  $t = 4$ , the variation in  $I_L$  is simulated and after 2 seconds the steady-state  $V$  is again similar to  $V^*$  (380V). In accordance with equation (5.5), the average voltage regulation objective is achieved. Moreover, greater oscillations in DGU currents imply greater peaks in the DGU voltage.

## Chapter 9: Discussion

This thesis provided new insights in the robustness of the proposed distributed controller by Trip et al. (2018) through introducing time delays in the communication network. Constant time delays in  $I_t$  and  $\theta$  measurements showed that delays over one of the two measurements could be handled by the system. However when simulating similar delays over both measurements simultaneously, the system showed instability.  $K$  is proven to be an effective control parameter on the boundaries of delays that can be handled by the system (Khalil et al., 2016). Without adjusting the control parameter  $K$ , the system showed no robustness against communication delays. However, this specific control parameter also has a great influence on oscillations during the transient. This is why all simulation results show transient behavior, which is not favourable regarding system's performance and reliability. Hence why the simulated graphs in chapter 7 show different behavior compared to the plots shown in Figure A.2. Lastly, the variation in  $I_L$  at  $t = 1s$  was shifted to  $t = 4s$  in order to demonstrate the controller response to variations in current demand.

For future research, the distributed control scheme should be modified in its equations to be able to react more stable when subjected to communication delays. In addition, time-varying delays can be implemented instead of constant time delays, since communication delays between neighbors may be time-varying and non-uniform because of protocol variations in the nature of data transmission or uncertainties and disturbances in communication channels (Ding et al., 2018). Furthermore, influences of possible packet losses are to be researched and included to bridge the gap between simulations and experiments. Moreover, an algorithm could be developed that adjusts the tuning parameters according to the scenario being applied to improve the performance of the system. Lastly, communication delays in combination with possible communication line failures could be researched in order to validate if the control scheme proposed by Trip et al. (2018) is stable under such circumstances.

## Chapter 10: Conclusion

In this Bachelor Integration Project, the distributed control scheme proposed by Trip et al. (2018) is subjected to communication delays in its communication lines. The influences of such delays are inevitable in a distributed control system and should thus be included in the design phase of a controller. By building the model in Simulink, simulations are executed in order to evaluate the performance of the distributed control scheme in terms of current sharing and average voltage regulation.

Firstly, implementing delays on  $I_t$  measurements was modeled. Simulations provide the insights that the system shows some robustness and both its control objectives are achieved. However, as the control parameter  $K$  must be adjusted in its value in order to achieve stability of the system, transient behavior is introduced. The greater the delay, the greater oscillations in generated currents and line currents are.

Secondly, delays on  $\theta$  measurements were investigated. The system was subjected to the same delays as in previous scenarios and showed again robustness to some extent. Current sharing and average voltage regulation were achieved. Important to note here is that from the simulation results, it is observed that the system shows more robustness against delays on  $\theta$  measurements than on  $I_t$  measurements which can be validated due to the fact that the influences of  $\theta$  throughout the control scheme are significantly lower than  $I_t$ , especially when the value of control parameter  $K$  is enlarged. Lastly, the control scheme was subjected to delays in both measurements ( $I_t$  and  $\theta$ ). Here, the system only showed robustness against communication delays when relatively small delays were simulated.

In all scenario's the control performance is somewhat poor since the system response is very oscillatory, reducing the system's performance and reliability. Hence, it can be concluded that even though including communication delays in the distributed control scheme designed Trip et al. (2018) is needed in order to make the DC microgrid more reliable, further research on the control scheme and its delays should be performed before the system is able to remain stable and limit its transient behavior when including communication delays.

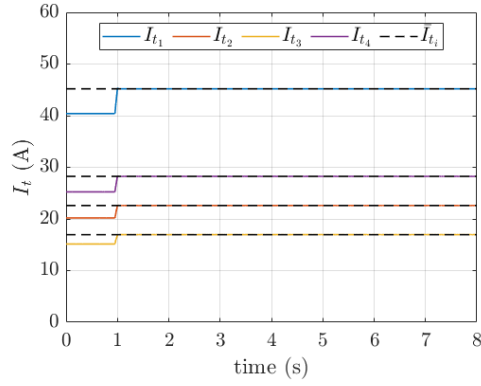
## Bibliography

- Allen-Prince, M., Thomas, C., and Yi, S. (2017). Analysis of the effects of communication delays for consensus of networked multi-agent systems. *International Journal of Control, Automation and Systems*, 15(5):2320–2328.
- Baros, D., Rigogiannis, N., Papanikolaou, N., and Loupis, M. (2020). Investigation of communication delay impact on dc microgrids with adaptive droop control. In *2020 International Symposium on Industrial Electronics and Applications (INDEL)*, pages 1–6. IEEE.
- Cucuzzella, M., Trip, S., De Persis, C., Cheng, X., Ferrara, A., and van der Schaft, A. (2018). A robust consensus algorithm for current sharing and voltage regulation in dc microgrids. *IEEE Transactions on Control Systems Technology*, 27(4):1583–1595.
- Delfino, F., Procopio, R., Rossi, M., Brignone, M., Robba, M., and Bracco, S. (2018). *Microgrid design and operation: toward smart energy in cities*. Artech House.
- Ding, L., Han, Q.-L., Sindi, E., et al. (2018). Distributed cooperative optimal control of dc microgrids with communication delays. *IEEE Transactions on Industrial Informatics*, 14(9):3924–3935.
- Dong, C., Guo, F., Jia, H., Xu, Y., Li, X., and Wang, P. (2017). Dc microgrid stability analysis considering time delay in the distributed control. *Energy Procedia*, 142:2126–2131.
- Du, Y., Tu, H., and Lukic, S. (2018). Distributed control strategy to achieve synchronized operation of an islanded mg. *IEEE Transactions on Smart Grid*, 10(4):4487–4496.
- Han, Y., Zhang, K., Li, H., Coelho, E. A. A., and Guerrero, J. M. (2017). Mas-based distributed coordinated control and optimization in microgrid and microgrid clusters: A comprehensive overview. *IEEE Transactions on Power Electronics*, 33(8):6488–6508.
- Kaur, A., Kaushal, J., and Basak, P. (2016). A review on microgrid central controller. *Renewable and Sustainable Energy Reviews*, 55:338–345.
- Khalil, A., Elkawafi, S., Elgaiyar, A. I., and Wang, J. (2016). Delay-dependent stability of dc microgrid with time-varying delay. In *2016 22nd international conference on automation and computing (ICAC)*, pages 360–365. IEEE.
- Kotpalliwar, S., Satpute, S., Meshram, S., Kazi, F., and Singh, N. (2015). Modelling and stability of time-delayed microgrid systems. *IFAC-PapersOnLine*, 48(30):294–299.
- Macana, C. A., Mojica-Nava, E., and Quijano, N. (2013). Time-delay effect on load frequency control for microgrids. In *2013 10th IEEE International Conference on Networking, Sensing and Control (ICNSC)*, pages 544–549. IEEE.
- Radwan, A. A. A. and Mohamed, Y. A.-R. I. (2014). Networked control and power management of ac/dc hybrid microgrids. *IEEE Systems Journal*, 11(3):1662–1673.

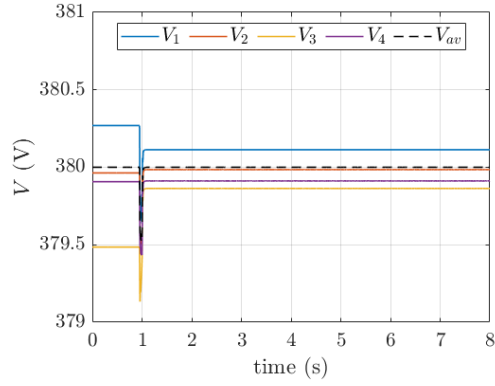
- Saleh, M., Esa, Y., and Mohamed, A. (2018). Effect of wireless communication delay on dc microgrids performance. In *2018 IEEE Energy Conversion Congress and Exposition (ECCE)*, pages 5164–5168. IEEE.
- Trip, S., Cucuzzella, M., Cheng, X., and Scherpen, J. (2018). Distributed averaging control for voltage regulation and current sharing in dc microgrids. *IEEE Control Systems Letters*, 3(1):174–179.
- Ustun, T. S., Ozansoy, C., and Ustun, A. (2012). Fault current coefficient and time delay assignment for microgrid protection system with central protection unit. *IEEE Transactions on power systems*, 28(2):598–606.
- Verschuren, P., Doorewaard, H., and Mellion, M. (2010). *Designing a research project*, volume 2. Eleven International Publishing The Hague.
- Zubieta, L. E. (2016). Are microgrids the future of energy?: Dc microgrids from concept to demonstration to deployment. *IEEE Electrification Magazine*, 4(2):37–44.



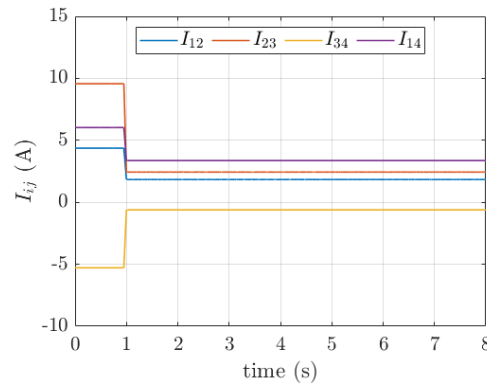
## A.2 Plots of generated currents, voltages, and line currents



(a) Plot of the generated currents in the DGUs



(b) Plot of the voltages in the DGUs



(c) Plot of the current in the line between the DGUs

Figure A.2: Simulation results (based on the article by Trip et al. (2018))

## Appendix B: Modeling with delays

### B.1 Simulink model with delays

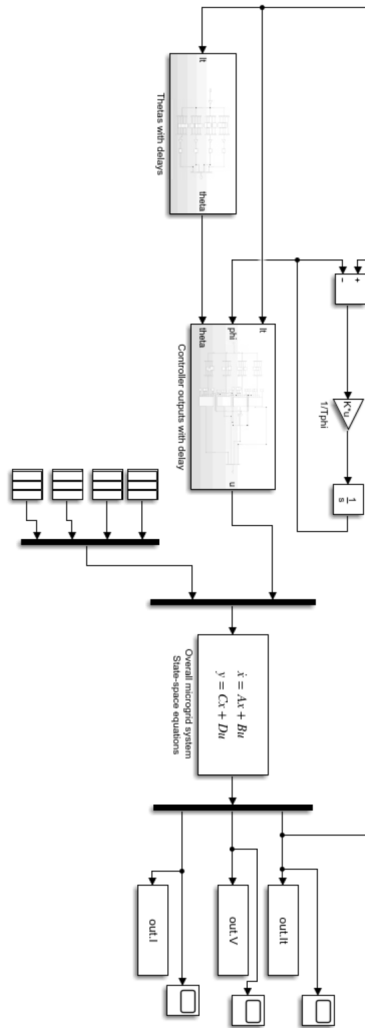


Figure B.1: Overview of the used Simulink model with delays

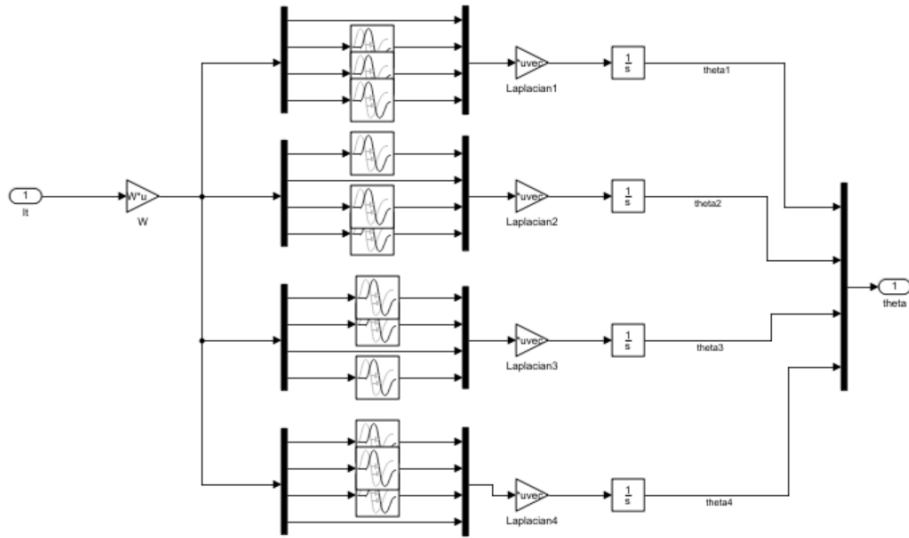


Figure B.2: Detailed overview of modeled delay over  $I_t$

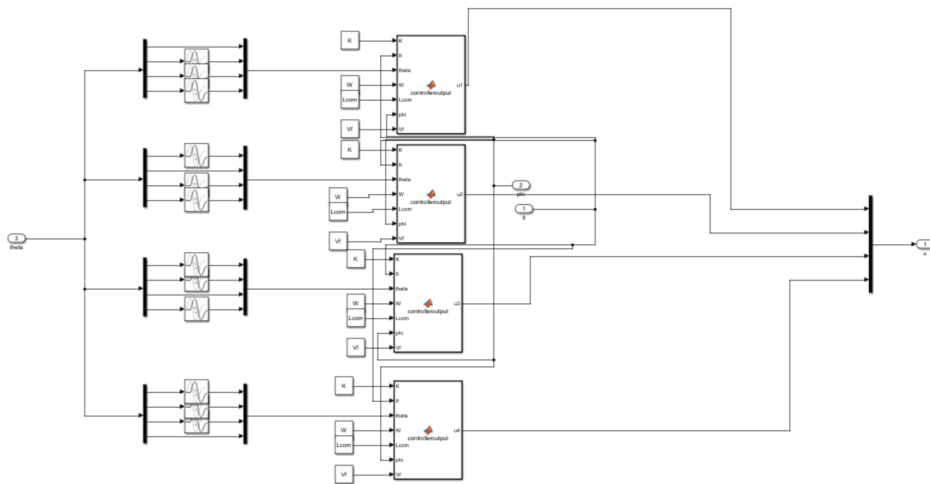


Figure B.3: Detailed overview of modeled delay over  $\theta$